LINEAR FINITE ELEMENTS MAY BE ONLY FIRST-ORDER POINTWISE ACCURATE ON ANISOTROPIC TRIANGULATIONS

NATALIA KOPTEVA

Abstract. We give a counterexample of an anisotropic triangulation on which the exact solution has a second-order error of linear interpolation, while the computed solution obtained using linear finite elements is only first-order pointwise accurate. Our example is given in the context of a singularly perturbed reaction-diffusion equation, whose exact solution exhibits a sharp boundary layer. Furthermore, we give a theoretical justification of the observed numerical phenomena using a finite-difference representation of the considered finite element methods. Both standard and lumped-mass cases are addressed.

1. Introduction

It appears that there is a perception in the finite-element community that the computed-solution error in the maximum norm is closely related to the corresponding interpolation error. While an almost best approximation property of finite-element solutions in the maximum norm has been rigourously proved (with a logarithmic factor in the case of linear elements) for some equations on quasi-uniform meshes [11, 12], there is no such result for strongly-anisotropic triangulations. Nevertheless, this perception is frequently considered a reasonable heuristic conjecture to be used in the anisotropic mesh adaptation [7, 6, 8, 4].

In this note we give a counterexample of an anisotropic triangulation on which

- the exact solution is in $C^\infty(\bar\Omega)$ and has a second-order pointwise error of linear interpolation $O(N^{-2})$,
- the computed solution obtained using linear finite elements is only first-order pointwise accurate, i.e. the pointwise error is as large as $O(N^{-1})$.

Here the maximum side length of mesh elements is $O(N^{-1})$ and the global number of mesh nodes does not exceed $O(N^2)$.

Our example is given in the context of singularly perturbed differential equations. Their solutions exhibit sharp boundary and interior layers, so locally anisotropic meshes (fine and anisotropic in layer regions and standard outside) are frequently employed in their numerical solution and, furthermore, have been shown to yield reliable numerical approximations in an efficient way (see, e.g., [5, 9, 13] and references in [10]).

Date: September 14, 2012 and, in revised form, October xx, 2012.

1991 *Mathematics Subject Classification.* Primary 65N15, 65N30, 65N50; Secondary 65N06.

Key words and phrases. Anisotropic triangulation, linear finite elements, maximum norm, singular perturbation, Bakhvalov mesh, Shishkin mesh.

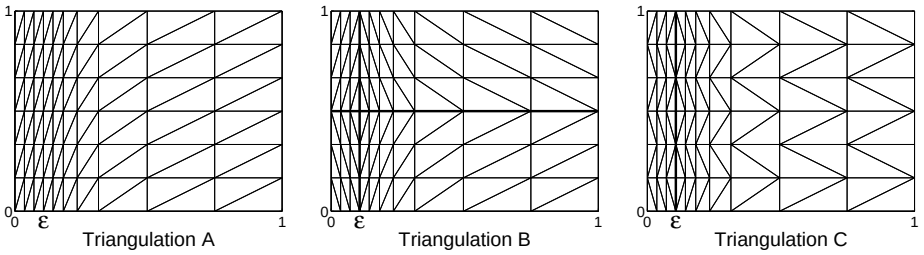

FIGURE 1. *Triangulations of types A, B and C.*

Example. Consider an exact solution $u(x,y) = e^{-x/\varepsilon}$ of the singularly perturbed reaction-diffusion problem

$$-\varepsilon^2\Delta u + u = 0 \quad \text{for } (x,y) \in \Omega, \qquad u = g \quad \text{for } (x,y) \in \partial\Omega, \tag{1.1}$$

where ε is a small positive parameter, $\Delta = \partial^2/\partial x^2 + \partial^2/\partial y^2$ is the Laplace operator, and the boundary data g matches the chosen exact solution. The domain Ω is a bounded polygonal domain. In particular we consider the cases of $\Omega = (0,1)^2$ and $\Omega := (0,2\varepsilon)\times(0,1)$, as well as a more general case of $\Omega \supset \mathring{\Omega} := (0,2\varepsilon)\times(-H,H)$, where $H = O(N^{-1})$.

The paper is organized as follows. In §2, problem (1.1) is solved numerically using both standard and lumped-mass linear finite elements. Triangulations of types A, B and C are considered that are obtained from standard layer-adapted tensor-product meshes by drawing diagonals as on Figure 1. In §3, we give a theoretical justification of the observed numerical phenomena using a finite-difference representation of the considered finite element methods.

Notation. We let C denote a generic positive constant that may take different values in different formulas, but is always independent of the mesh and ε. A subscripted C (e.g., C_1) denotes a positive constant that is independent of N and ε and takes a fixed value. Notation $v = O(w)$ will be used for $C^{-1}w \le v \le Cw$, while $v = \mathcal{O}(w)$ will denote $|v| \le Cw$, with some constant C.

2. Numerical Results

Consider a tensor-product of a layer-adapted mesh $\{x_i\}_{i=0}^N$ in the x-direction and the uniform mesh $\{\frac{j}{M}\}_{j=0}^M$ in the y-direction, where $M = O(N)$. Whenever $\Omega = (0,1)^2$, the mesh $\{x_i\}$ will be a version of the Bakhvalov mesh [2] or the Shishkin mesh [13] described below. Whenever $\Omega = (0,2\varepsilon)\times(0,1)$, the mesh $\{x_i\}$ will be uniform.

Bakhvalov mesh [2] For some $\gamma \in (0,1)$, set $\sigma := 2\varepsilon(\gamma^{-1}|\ln\varepsilon| + 1)$ and assume that ε is sufficiently small for $\sigma \in (0,1)$. Now define the mesh $\{x_i\}_{i=0}^{N/2}$ on $[0,\sigma]$ by

$$x_i := x\big([1+\gamma-\varepsilon]\,\tfrac{2i}{N}\big), \quad x(t) := \begin{cases} 2\varepsilon\,\gamma^{-1}t, & t \in [0,\gamma] \\ 2\varepsilon\,[1-\gamma^{-1}\ln(1+\gamma-t)], & t \in [\gamma, 1+\gamma-\varepsilon] \end{cases}.$$

The remaining part of the mesh $\{x_i\}_{i=N/2}^N$ on $[\sigma,1]$ is uniform. In fact, one can easily see that on $[0,2\varepsilon]$ this mesh is also uniform, with $x_i - x_{i-1} = O(\varepsilon N^{-1})$.

Shishkin mesh [13] For some $\gamma \in (0,1)$, set $\sigma = 2\gamma^{-1}\varepsilon\ln\frac{N}{2}$. Now construct a piecewise-uniform mesh by dividing the intervals $[0,\sigma]$ and $[\sigma,1]$ into N_1 and $N-N_1$ equal subintervals for some $N_1 = O(N)$.

TABLE 1. Bakhvalov tensor-product mesh, $\gamma = 0.8$, $M = \frac{1}{4}N$: maximum nodal errors and computational rates r in $(N^{-1})^r$.

		Triangulation A			Triangulation B		
	N	$\varepsilon = 2^{-8}$	$\varepsilon = 2^{-16}$	$\varepsilon = 2^{-24}$	$\varepsilon = 2^{-8}$	$\varepsilon = 2^{-16}$	$\varepsilon = 2^{-24}$
Lumped Masses	32	1.065e-3	1.070e-3	1.070e-3	1.543e-2	1.545e-2	1.545e-2
		1.99	1.99	1.99	1.07	1.07	1.07
	64	2.685e-4	2.697e-4	2.697e-4	7.328e-3	7.353e-3	7.353e-3
		2.00	2.00	2.00	0.98	0.97	0.97
	128	6.726e-5	6.756e-5	6.756e-5	3.713e-3	3.757e-3	3.757e-3
		2.00	2.00	2.00	1.03	0.99	0.99
	256	1.684e-5	1.691e-5	1.691e-5	1.818e-3	1.897e-3	1.897e-3
No Mass Lumping	32	1.422e-3	1.430e-3	1.430e-3	1.718e-2	1.723e-2	1.723e-2
		2.01	2.01	2.01	0.97	0.97	0.97
	64	3.526e-4	3.554e-4	3.554e-4	8.754e-3	8.811e-3	8.811e-3
		2.02	2.00	2.00	0.98	0.96	0.96
	128	8.710e-5	8.873e-5	8.873e-5	4.443e-3	4.527e-3	4.527e-3
		2.05	2.00	2.00	1.04	0.98	0.98
	256	2.097e-5	2.217e-5	2.217e-5	2.156e-3	2.292e-3	2.292e-3

Remark 2.1 (Interpolation error). A calculation shows that the linear interpolation error of our exact solution $u = e^{-x/\varepsilon}$ on any of the Triangulations A, B or C is $O\big(N^{-1}\ln^p \frac{N}{2}\big)^r$ in the maximum norm, where $p = 0$ if the Bakhvalov mesh is used or the uniform mesh in the domain $\Omega = (0, 2\varepsilon) \times (0, 1)$, and $p = 1$ if the Shishkin mesh is used. Interestingly, one gets a similar second-order bound (with a logarithmic factor in the case of the Shishkin mesh) for the error of the standard five-point difference scheme applied to problem (1.1) on the corresponding tensor-produce mesh (see, e.g., [5, 9]).

Tables 1–3 give the maximum nodal errors (odd rows) and the computational convergence rates r in $(N^{-1}\ln^p \frac{N}{2})^r$ (even rows) for Triangulations A and B obtained from the three tensor-product meshes. For the considered values of ε, these meshes are highly anisotropic; for example, in the case of the Bakhvalov mesh (see Table 1), the mesh aspect ratio changes between 2 away from the layer and $(2.25\,\varepsilon)^{-1}$ in the layer region. The numerical results for the standard finite elements are quite similar to the case of mass lumping, so we consider both cases only in Table 1.

We observe that whenever Triangulation A is used, one gets a second-order accuracy, with a logarithmic factor in the case of the Shishkin mesh (similar to the accuracy of the five-point finite-difference scheme, which, in fact, is identical with the lumped-mass finite elements on Triangulation A). However, when one switches to Triangulation B, linear finite elements become only (almost) first-order pointwise accurate in contrast to the (almost) second-order accuracy of the interpolation error. Triangulation C also yields only (almost) first-order convergence (see also Remark 3.5 and Figure 3). In summary, we conclude that

- when Triangulations B and C are used, linear finite elements are only first-order pointwise accurate;
- the order of convergence dramatically deteriorates from 2 to 1 as one switches from Triangulation A to Triangulation B or C.

TABLE 2. Shishkin mesh, $\gamma = 0.9$, $M = \frac{1}{4}N$, $N_1 = \frac{3}{4}N$: maximum nodal errors and computational rates r in $(N^{-1} \ln \frac{N}{2})^r$

	N	Triangulation A $\varepsilon = 2^{-8}$	$\varepsilon = 2^{-16}$	$\varepsilon = 2^{-24}$	Triangulation B $\varepsilon = 2^{-8}$	$\varepsilon = 2^{-16}$	$\varepsilon = 2^{-24}$
Lumped Masses	32	1.850e-3	2.109e-3	2.109e-3	1.477e-2	1.478e-2	1.478e-2
		3.295	3.278	3.277	1.222	1.217	1.217
	64	3.930e-4	4.516e-4	4.521e-4	8.317e-3	8.340e-3	8.340e-3
		1.995	2.268	2.269	0.977	0.962	0.962
	128	1.418e-4	1.418e-4	1.418e-4	5.048e-3	5.103e-3	5.103e-3
		1.998	1.997	1.997	1.023	0.969	0.969
	256	4.832e-5	4.832e-5	4.832e-5	2.908e-3	3.027e-3	3.027e-3

TABLE 3. Uniform mesh in $(0, 2\varepsilon) \times (0, 1)$, $M = \frac{1}{4}N$: maximum nodal errors and computational rates r in $(N^{-1})^r$

	N	Triangulation A $\varepsilon = 2^{-8}$	$\varepsilon = 2^{-16}$	$\varepsilon = 2^{-24}$	Triangulation B $\varepsilon = 2^{-8}$	$\varepsilon = 2^{-16}$	$\varepsilon = 2^{-24}$
Lumped Masses	32	4.767e-5	4.767e-5	4.767e-5	2.985e-3	2.986e-3	2.986e-3
		1.998	1.998	1.998	1.018	1.016	1.016
	64	1.193e-5	1.193e-5	1.193e-5	1.474e-3	1.476e-3	1.476e-3
		2.000	2.000	2.000	1.016	1.008	1.008
	128	2.983e-6	2.983e-6	2.983e-6	7.288e-4	7.339e-4	7.339e-4
		2.000	2.000	2.000	1.033	1.004	1.004
	256	7.458e-7	7.458e-7	7.458e-7	3.561e-4	3.659e-4	3.659e-4

3. Theoretical Justification

To understand the numerical phenomena described in the previous section, we represent the considered finite elements as finite-difference schemes on the underlying rectangular tensor-product meshes.

Suppose $\Omega \supset \mathring{\Omega}$, where the subdomain $\mathring{\Omega}$ and the tensor-product mesh $\mathring{\omega}_h$ in this subdomain are defined by

$$\mathring{\Omega} := (0, 2\varepsilon) \times (-H, H), \quad \mathring{\omega}_h := \{x_i = hi\}_{i=0}^{2N_0} \times \{-H, 0, H\}, \quad h = \tfrac{\varepsilon}{N_0}. \tag{3.1}$$

The triangulation $\mathring{\mathcal{T}}$ in $\mathring{\Omega}$ is obtained by drawing diagonals in each rectangle as shown on Figure 2, using the mesh transition point $(\varepsilon, 0)$.

Next, let U be the piecewise-linear finite-element solution obtained on some triangulation $\mathcal{T} \supset \mathring{\mathcal{T}}$ in the global domain Ω, for whose nodal values in $\mathring{\Omega}$ we use the notation

$$U_i := U(x_i, 0), \qquad U_i^{\pm} := U(x_i, \pm H).$$

Now a calculation yields a finite-difference representation in the *lumped-mass* case:

$$\mathcal{L}^h U(x_i, 0) := \tfrac{\varepsilon^2}{h^2}[-U_{i-1} + 2U_i - U_{i+1}] + \tfrac{\varepsilon^2}{H^2}[-U_i^- + 2U_i - U_i^+] + \gamma_i U_i = 0 \tag{3.2a}$$

for $i = 1, \dots, 2N_0 - 1$, where

$$\gamma_i = 1 \quad \text{for } i \neq N_0, \qquad \gamma_{N_0} = \tfrac{2}{3}. \tag{3.2b}$$

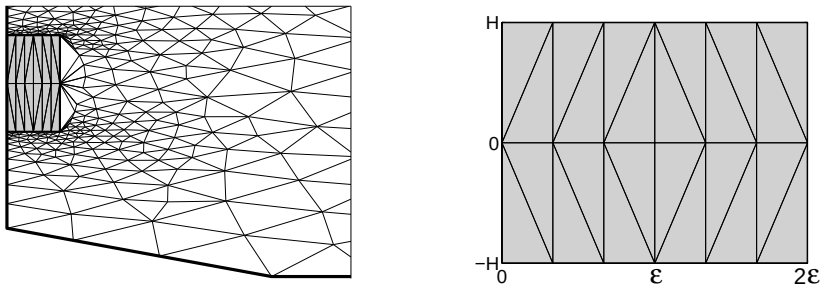

FIGURE 2. *Triangulation in Ω; right-hand picture enlarges the subdomain $\mathring{\Omega}$.*

In the *standard (non-lumped-mass)* case, one gets a similar finite-difference representation for $i = 1, \ldots, 2N_0 - 1$:

$$\tilde{\mathcal{L}}^h U_(x_i, 0) := \mathcal{L}^h U_i - \tfrac{1}{12} \sum_{(x',y') \in \mathcal{S}_i} [U_i - U(x', y')] = 0, \tag{3.3}$$

where $\mathcal{S}_i$ denotes the set of meshnodes that have a common edge with $(x_i, 0)$.

Remark 3.1. Note that if γ_i in (3.2a) is replaced by 1, one gets the standard five-point difference scheme for equation (1.1), for which, using the discrete maximum principle, one can easily show that if a tensor-product mesh of type $\mathring{\omega}_h$ is used in the entire domain Ω, then the nodal error is $O\big(\frac{h^2}{\varepsilon^2}\big)$. Our method differs from this difference scheme at one point $(x_{N_0}, 0)$, where $\gamma_i = \frac{2}{3}$, i.e. at this point, compared to the second-order finite-difference method, we have a truncation error $O(1)$. As we show in Lemma 3.3 below, this results in the deterioration of pointwise accuracy of the computed solution to $O\big(\frac{h}{\varepsilon}\big)$.

Remark 3.2. A triangulation, similar to Triangulation B on Figure 1 (and also to triangulation $\mathring{\mathcal{T}}$ on Figure 2), but obtained from a uniform tensor-product mesh, has been used to show that the logarithmic factor in the L_∞-norm error estimate for linear finite elements applied to the Laplace equation is sharp [3, 1]. Our approach is, in fact, similar to that in [1] in that we represent a finite element method as a finite-difference scheme to get a lower bound for the error.

We shall consider the lumped-mass and non-lumped-mass cases separately.

3.1. **Lumped-Mass Linear Finite Elements.**

Lemma 3.3 (Lumped-mass case)**.** *Let $u = e^{-x/\varepsilon}$ be the exact solution of problem (1.1) posed in a domain $\Omega \supset \mathring{\Omega}$, a triangulation $\mathcal{T}$ in Ω be such that $\mathcal{T} \supset \mathring{\mathcal{T}}$ subject to the definitions (3.1), and U be the computed solution obtained using lumped-mass linear finite elements. There exist sufficiently small constants C_0, C_1 and C_2 such that if $N_0^{-1} \le C_1$ and $\frac{\varepsilon^2}{H^2} \le C_2 N_0^{-1}$, then*

$$\max_{\bar{\Omega}} |U - u| \ge C_0 N_0^{-1}. \tag{3.4}$$

Proof. (i) First, consider the auxiliary piecewise-linear computed solution $\mathring{U}$ obtained on the triangulation $\mathring{\mathcal{T}}$ in the subdomain $\mathring{\Omega}$, subject to the boundary conditions $\mathring{U}(x', y') = u(x', y')$ at each meshnode $(x', y') \in \partial\mathring{\Omega}$. At the interior meshnodes, $\mathring{U}$ satisfies (3.2a), i.e. $\mathcal{L}^h \mathring{U}(x_i, 0) = 0$ for $i = 1, \ldots, 2N_0 - 1$. We shall now

prove that, for a sufficiently small constant C_0, one has

$$[\mathring{U} - u](x_{N_0}, 0) \geq 2C_0 N_0^{-1}. \tag{3.5}$$

By the discrete maximum principle, $0 \leq \mathring{U} \leq 1$, so $\mathcal{L}^h \mathring{U}(x_i, 0) = 0$ can be rewritten as a one-dimensional discrete equation for the unknown vector $\{\mathring{U}_i\}_{i=0}^{2N_0}$

$$L_x^h \mathring{U}_i = \tfrac{\varepsilon^2}{h^2}[-\mathring{U}_{i-1} + 2\mathring{U}_i - \mathring{U}_{i+1}] + \gamma_i \mathring{U}_i = \mathcal{O}\big(\tfrac{\varepsilon^2}{H^2}\big), \tag{3.6}$$

where $\mathring{U}_i := \mathring{U}(x_i, 0)$, subject to the boundary conditions $\mathring{U}_0 = u(0,0)$ and $\mathring{U}_{2N_0} = u(2\varepsilon, 0)$. The truncation error for this equation is

$$L_x^h\,[\mathring{U}_i - u(x_i,0)] = [1-\gamma_i]\,u(x_i,0) + \mathcal{O}\big(\tfrac{\varepsilon^2}{H^2} + \tfrac{h^2}{\varepsilon^2}\big). \tag{3.7}$$

Here, by virtue of (3.2b), $[1-\gamma_i]u(x_i,0) = [\frac{1}{3}\delta_{iN_0}]e^{-x_i/\varepsilon} = \frac{1}{3}e^{-1}\delta_{iN_0}$, where δ_{iN_0} denotes the Kronecker delta. As L_x^h satisfies the discrete maximum principle, now (3.7) yields the representation

$$\mathring{U}_i - u(x_i,0) = \tfrac{1}{3}e^{-1} h\, G_i^h + \mathcal{O}\big(\tfrac{\varepsilon^2}{H^2} + \tfrac{h^2}{\varepsilon^2}\big). \tag{3.8}$$

Here G_i^h is the discrete Green's function of the one-dimensional operator L_x^h that satisfies $L_x^h G_i^h = h^{-1}\delta_{iN_0}$ for $i = 1, \dots, 2N_0 - 1$, subject to $G_0^h = G_{2N_0}^h = 0$. To complete the proof of (3.5), it now suffices to show that $G_{N_0}^h \geq C_4 \varepsilon^{-1}$ for some constant C_4; then one simply needs to choose sufficiently small constants C_0, C_1 and C_2 such that $\frac{1}{3}e^{-1}C_4\frac{h}{\varepsilon} + \mathcal{O}\big(\frac{\varepsilon^2}{H^2} + \frac{h^2}{\varepsilon^2}\big) \geq 2C_0\frac{h}{\varepsilon}$.

To bound $G_{N_0}^h$, note that $G_i^h = G_{2N_0-i}^h$ and $G_i^h = G_{N_0}^h[w(x_i) + \mathcal{O}(\frac{h^2}{\varepsilon^2})]$ for $i \leq N_0$, where $w(x)$ solves the equation $-\varepsilon^2 w'' + w = 0$ subject to $w(0) = 0$ and $w(1) = 1$. This implies that $\rho := \frac{\varepsilon}{h}[G_{N_0}^h - G_{N_0\pm1}^h]/G_{N_0}^h \leq C_5$ for some constant C_5. Now, $L_x^h G_{N_0}^h = h^{-1}$ can be rewritten as $G_{N_0}^h[2\frac{\varepsilon}{h}\rho + \frac{2}{3}] = h^{-1}$ or, equivalently, $G_{N_0}^h[2\rho + \frac{2}{3}\frac{h}{\varepsilon}] = \varepsilon^{-1}$. As $\frac{h}{\varepsilon} \leq C_1$ and $\rho \geq C_5$, choosing C_1 sufficiently small we get $G_{N_0}^h \geq C_4\varepsilon^{-1}$ with $C_4 := (3C_4)^{-1}$, and, hence, the desired bound (3.5).

(ii) In view of (3.5), to establish (3.4), it suffices to show that

$$\max_{\bar\Omega} |U - u^I| \geq \tfrac{1}{2} \max_{\mathring\Omega} |\mathring{U} - u^I| =: \tfrac{1}{2}\mathring{e}, \tag{3.9}$$

where u^I is the standard piecewise-linear interpolant of u.

Let $Z := U - \mathring{U}$ in $\mathring\Omega$ and $Z_{\max} := \sup_{\mathring\Omega}|Z|$. Note that $\mathcal{L}^h Z(x_i, 0) = 0$ and $Z = U - u^I$ on $\partial\mathring\Omega$. As, by the discrete maximum principle, $|Z|$ attains its maximum on $\partial\mathring\Omega$, so $\max_{\partial\mathring\Omega}|U - u^I| = Z_{\max}$. On the other hand, $U - u^I = (\mathring{U} - u^I) + Z$ yields $\max_{\mathring\Omega}|U - u^I| \geq \mathring{e} - Z_{\max}$ As the maximum of the two values $\mathring{e} - Z_{\max}$ and $Z_{\max}$ exceeds their average, the desired relation (3.9) follows. □

Remark 3.4. As we only consider $\varepsilon \ll N^{-1}$, Lemma 3.3 applies to all triangulations of type B used in Tables 1–3, with $N_0^{-1} = O(N^{-1}\ln^p\frac{N}{2})$, where $p = 0$ if the Bakhvalov mesh is used or the uniform mesh in the domain $\Omega = (0, 2\varepsilon) \times (0, 1)$, and $p = 1$ if the Shishkin mesh is used. Furthermore, this lemma still applies if one switches from Triangulation B to Triangulation C.

Remark 3.5. A version of part (i) of the proof of Lemma 3.3 can be applied to the global Triangulation B in Ω to show that $|[U-u](x,y)| \leq C(N^{-1}\ln^p\frac{N}{2})^2$ whenever $|y - \frac{1}{2}| \geq M^{-1}$, i.e. the deterioration in the accuracy occurs only near $y = \frac{1}{2}$; see Figure 3 (left). However, as Figure 3 (right) demonstrates, if one switches to Triangulation C, the error of order (almost) 1 becomes spread throughout the boundary-layer region.

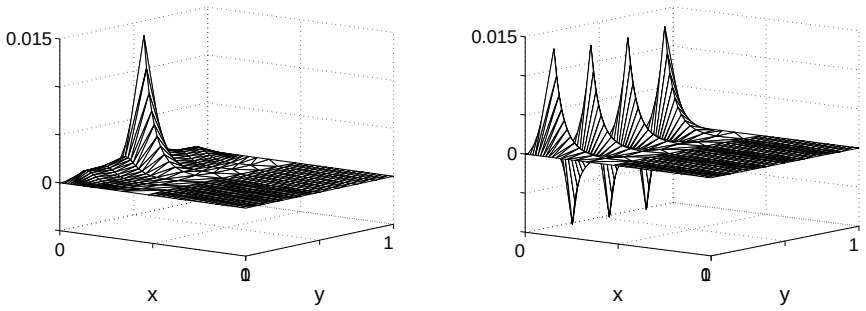

FIGURE 3. *Pointwise computed-solution error on Triangulation B (left) and C (right), Bakhvalov tensor-product mesh,* $\varepsilon = 0.05$*,* $N = 32$*,* $M = \frac{1}{4}N$*,* $\gamma = 0.8$*.*

3.2. **Standard Linear Finite Elements.**

Lemma 3.6 (Non-lumped-mass case)**.** *The statement of Lemma 3.3 remains valid for the computed solution* U *obtained using standard linear finite elements.*

Proof. We imitate the proof of Lemma 3.3 with a few changes described below.

(i) This part of the proof is devoted to establishing (3.5), only now $\mathring{U}(x_i,0)$ satisfies (3.3), i.e. $\tilde{\mathcal{L}}^h\mathring{U}(x_i,0) = 0$ for $i = 1,\dots,2N_0-1$. Consider another auxiliary piecewise-linear function $\mathring{V}$ that satisfies the same boundary conditions as $\mathring{U}$, i.e. $\mathring{V}(x',y') = u(x',y')$ at each meshnode $(x',y') \in \partial\mathring{\Omega}$, and the discrete relations

$$\bar{\mathcal{L}}^h\mathring{V}(x_i,0) = \big[\mathcal{L}^h\mathring{V}_i - \tfrac{1}{12}(-\mathring{V}_{i-1} + 2\mathring{V}_i - \mathring{V}_{i+1})\big] = 0$$

for $i = 1,\dots,2N_0-1$, with the standard notation $\mathring{V}_i := \mathring{V}(x_i,0)$. Here the operator $\bar{\mathcal{L}}^h$ is somewhat between $\mathcal{L}^h$ and $\tilde{\mathcal{L}}^h$; in fact, $\bar{\mathcal{L}}^h$ is a slightly perturbed version of $\mathcal{L}^h$ of (3.2a) obtained by replacing $\frac{\varepsilon^2}{h^2}$ with $\frac{\varepsilon^2}{h^2} - \frac{1}{12} = \frac{\varepsilon^2}{h^2}\big[1 - \frac{h^2}{12\varepsilon^2}\big]$, where $\frac{h}{\varepsilon}$ is assumed sufficiently small. Consequently, a version of (3.5) is valid with $\mathring{V}$ replacing $\mathring{U}$ (and a different constant C_0), as well as a version of (3.8).

It remains to get a suitable lower bound on $(\mathring{U} - \mathring{V})_{N_0}$. A calculation using the definition of $\tilde{\mathcal{L}}^h$ in(3.3) and the structure of the mesh (see Figure 2) yields

$$\tilde{\mathcal{L}}^h\mathring{V}_i = \bar{\mathcal{L}}^h\mathring{V}_i - \tfrac{1}{12}\mathcal{A}\mathring{V}_i - \hat{\alpha}_i\tfrac{1}{12}[\mathcal{A}\mathring{V}_{i+1} + 2(\mathring{V}_i - \mathring{V}_{i+1})] - \check{\alpha}_i\tfrac{1}{12}[\mathcal{A}\mathring{V}_{i-1} + 2(\mathring{V}_i - \mathring{V}_{i-1})],$$

where, with the standard notation $\mathring{V}_i^{\pm} := \mathring{V}(x_i,\pm H)$,

$$\mathcal{A}\mathring{V}_i := -\mathring{V}_i^- + 2\mathring{V}_i - \mathring{V}_i^+, \qquad \hat{\alpha}_i := \begin{cases} 1, & i < N_0 \\ 0, & i \ge N_0 \end{cases}, \quad \check{\alpha}_i := \begin{cases} 0, & i \le N_0 \\ 1, & i > N_0 \end{cases}.$$

Now, as $\tilde{\mathcal{L}}^h[\mathring{U}_i - \mathring{V}_i] = [\bar{\mathcal{L}}^h - \tilde{\mathcal{L}}^h]\mathring{V}_i$, one easily gets

$$\tilde{\mathcal{L}}^h[\mathring{U}_i - \mathring{V}_i] = \tfrac{1}{12}\big[\mathcal{A}\mathring{V}_i + \hat{\alpha}_i\mathcal{A}\mathring{V}_{i+1} + \check{\alpha}_i\mathcal{A}\mathring{V}_{i-1}\big] + \tfrac{1}{6}F_i \tag{3.10}$$

for $i = 1,\dots,2N_0-1$, with

$$F_i := \hat{\alpha}_i(\mathring{V}_i - \mathring{V}_{i+1}) + \check{\alpha}_i(\mathring{V}_i - \mathring{V}_{i-1}).$$

Note that $\tilde{\mathcal{L}}^h[\mathring{U}_i - \mathring{V}_i]$ in (3.10) involves the values $\mathring{U}_i^{\pm} - \mathring{V}_i^{\pm} = 0$, so this discrete equation may be interpreted as a one-dimensional discrete equation for the unknown vector $\{\mathring{U}_i - \mathring{V}_i\}_{i=0}^{2N_0}$. In this interpretation, (3.10) satisfies the discrete maximum principle.

Next, to consider the right-hand side in (3.10), set $\varrho := \frac{\varepsilon^2}{H^2} + \frac{h^2}{\varepsilon^2}$. Recall that $\mathring{V}_i^{\pm} = u(x_i, \pm H) = u(x_i, 0)$, while for $\mathring{V}_i$ we have a version of (3.8) that involves $G_i^h \ge 0$, so $\mathcal{A}\mathring{V}_i \ge -\mathcal{O}(\varrho)$. For F_i, define a decomposition $F_i = F_i' + F_i''$ by

$$F_i' := \begin{cases} -F_{2N_0-i}, & i \le N_0 \\ F_i, & i \ge N_0 \end{cases} \quad \Rightarrow \; F - F_i' = \hat{\alpha}_i \big[(\mathring{V}_i - \mathring{V}_{i+1}) + (\mathring{V}_{2N_0-i} - \mathring{V}_{2N_0-i-1}) \big].$$

Here, a version of (3.6) for $\mathring{V}$ can be used to deduce that $F_i'' \ge -\mathcal{O}\big(\frac{\varepsilon^2}{H^2}\frac{h^2}{\varepsilon^2} N_0\big) \ge -\mathcal{O}(\varrho)$. To deal with F_i', let $\tilde{\mathcal{L}}^h e_i' = F_i'$ subject to $e' = 0$ at the meshnodes on $\partial\mathring{\Omega}$. The symmetry of this problem combined with the symmetry of F_i' immediately implies that $e_{N_0}' = 0$. Finally, using our observations on the ingredients of the right-hand side in (3.10), we conclude that $\tilde{\mathcal{L}}^h[\mathring{U}_i - \mathring{V}_i - e_i'] \ge -\mathcal{O}(\varrho)$. So, by the discrete maximum principle, one has $\mathring{U}_i - \mathring{V}_i - e_i' \ge -\mathcal{O}(\varrho)$, so $\mathring{U}_{N_0} - \mathring{V}_{N_0} \ge -\mathcal{O}\big(\frac{\varepsilon^2}{H^2} + \frac{h^2}{\varepsilon^2}\big)$. Combining this with a version of (3.5) for $\mathring{V}$, one finally gets the desired bound (3.5) for $\mathring{U}$ (with a different C_0).

(ii) This part of the proof is identical with part (ii) in the proof of Lemma 3.3. To show that $|Z|$ attains its maximum on $\partial\mathring{\Omega}$, move the terms $Z_i^{\pm}$, available from the boundary data, to the right-hand side in the discrete equation $\tilde{\mathcal{L}}^h Z = 0$. The resulting nonhomogeneous one-dimensional discrete equation for the unknown vector $\{Z_i\}_{i=0}^{2N_0}$ satisfies the discrete maximum principle, which can be used to deduce that the maximum of $|Z|$ indeed occurs on $\partial\mathring{\Omega}$. □

References

[1] V. B. Andreev, *The logarithmic factor in the L_∞-norm error estimate for linear finite elements is sharp*, Semin. I. Vekua Inst. Appl. Math. Rep. (Dokl. Semin. Inst. Prikl. Mat. im. I. N. Vekua), 4 (1989), no. 3, 17–20 (in Russian).

[2] N. S. Bakhvalov, On the optimization of methods for solving boundary value problems with boundary layers, Zh. Vychisl. Mat. Mat. Fis., 9 (1969), 841–859 (in Russian).

[3] H. Blum, Q. Lin and R. Rannacher, *Asymptotic error expansion and Richardson extrapolation for linear finite elements*, Numer. Math. 49 (1986), 11–37.

[4] L. Chen, P. Sun, J. Xu, *Optimal anisotropic meshes for minimizing interpolation errors in L^p-norm*, Math. Comp. 76 (2007), 179–204.

[5] C. Clavero, J. L. Gracia and E. O'Riordan, *A parameter robust numerical method for a two dimensional reaction-diffusion problem*, Math. Comp., 74 (2005), 1743–1758.

[6] E. F. D'Azevedo, *Optimal triangular mesh generation by coordinate transformation*, SIAM J. Sci. Statist. Comput., 12 (1991), 755–786.

[7] E. F. D'Azevedo and R. B. Simpson, *On optimal interpolation triangle incidences*, SIAM J. Sci. Statist. Comput., 10 (1989), 1063–1075.

[8] V. Dolejší, J. Felcman, *Anisotropic mesh adaptation for numerical solution of boundary value problems*, Numer. Methods Partial Differential Equations, 20 (2004), 576–608.

[9] N. Kopteva, *Maximum norm error analysis of a 2d singularly perturbed semilinear reaction-diffusion problem*, Math. Comp., 76 (2007), 631–646.

[10] H.-G. Roos, M. Stynes and L. Tobiska, *Robust Numerical Methods for Singularly Perturbed Differential Equations*, Springer, Berlin, 2008.

[11] A. H. Schatz and L. B. Wahlbin, *On the quasi-optimality in L_∞ of the $\mathring{H}^1$-projection into finite element spaces*, Math. Comp. 38 (1982), 1–22.

[12] A. H. Schatz and L. B. Wahlbin, *On the finite element method for singularly perturbed reaction-diffusion problems in two and one dimensions*, Math. Comp., 40 (1983), 47–89.

[13] G. I. Shishkin, *Grid approximation of singularly perturbed elliptic and parabolic equations*, Ur. O. Ran, Ekaterinburg, 1992 (in Russian).

Department of Mathematics and Statistics, University of Limerick, Limerick, Ireland
E-mail address: natalia.kopteva@ul.ie